Numerical simulation of natural convection in a concentric annulus between a square outer cylinder and a circular inner cylinder using the Taylor-series-expansion and least-squares-based lattice Boltzmann method

Y. Peng, Y. T. Chew, and C. Shu
Department of Mechanical Engineering, National University of Singapore, 10 Kent Ridge Crescent, Singapore 119260
(Received 24 April 2002; revised manuscript received 16 September 2002; published 5 February 2003)

In this paper, natural convective heat transfer in a horizontal concentric annulus between a square outer cylinder and a heated circular inner cylinder is numerically studied using the Taylor-series-expansion and least-squares-based lattice Boltzmann method (TLLBM). The TLLBM is used to extend the current thermal model to more practical applications. Since the TLLBM is basically a meshless approach and can be applied to any complex geometry, we can easily use it to solve the complex thermal problem accurately and effectively. The present method is validated by comparing its numerical results with available data in the literature, and very good agreement has been achieved.

DOI: 10.1103/PhysRevE.67.026701 PACS number(s): 83.85.Pt, 45.50.−j, 47.11.+j

I. INTRODUCTION

The lattice Boltzmann method (LBM) has been developed into an attractive numerical scheme in the last ten years [1]. However, it lags behind conventional computational fluid dynamics methods for the simulation of fluid flows in realistically complicated geometries. Various methods have been proposed to remedy this unsatisfactory state of affairs. So far, there are mainly two ways to improve the standard LBM. One is based on the discrete Boltzmann equation, which is solved by using traditional finite-difference method [2] and finite-volume method [3–8] on the general coordinate system. The other one is the time-dependent interpolation scheme by adhering to the Lagrangian form of the LBE. This scheme was proposed by He *et al.* [9]. It has been shown that both ways are successful in simulating different fluid systems on complex geometries. However, the finite-volume LBM and finite-difference LBM have the disadvantage of numerical diffusion. The interpolation-supplemented LBE [9] model successfully overcomes the above shortcoming by preserving the time accuracy of the traditional LBE. The price to pay is the need of interpolation between the spatial grid and particle positions. To avoid spurious numerical viscosity, a second-order upwind interpolation scheme is used. This model has proved its viability for a two-dimensional flow past a cylinder using cylindrical coordinates, at both low and high Reynolds numbers. However, it has an extra computational effort for interpolation at every time step, and it also has a strict restriction on the selection of interpolation points, which requires upwind 9 points for two-dimensional problems and upwind 27 points for three-dimensional problems if a structured mesh is used.

In order to implement the LBE more efficiently for flows with arbitrary geometry, a version of the LBM, which is based on the standard LBM, the well-known Taylor-series-expansion and least-squares approach, was proposed by Shu *et al.* [10]. The final form is an algebraic formulation, in which the coefficients only depend on the coordinates of mesh points and lattice velocity, and can be computed in advance. This method is also free of lattice models. Numerical experiments on isothermal flows showed that this method is an efficient and flexible approach for practical applications.

Due to the same reason as in the isothermal flow and the complexity of the thermal problem itself, the current thermal LBM is restricted to the regular grid, which hinders its application to practical problems such as natural convection in an enclosed space. In practice, the flow and thermal fields in different kinds of enclosed space are of great importance due to their wide applications such as in solar collector receivers, insulation and flooding protection for buried pipes used for district heating and cooling, cooling systems in nuclear reactors, etc. A large number of literatures were published in the past few decades for this kind of problems. For concentric and eccentric cases in a horizontal annulus between two circular cylinders, the flow and thermal fields have been well studied. Comparatively, little work has been conducted in more complex domains, such as the annulus between a square outer cylinder and a circular inner cylinder. In this paper, we will show that the Taylor-series-expansion and least-squares-based LBM (TLLBM) together with the current thermal model can provide very accurate results for these kinds of complex thermal problems.

II. METHODOLOGY

A. Taylor-series expansion and least-squares-based LBM

The TLLBM is based on the well-known fact that the distribution function is a continuous function in physical space and can be well defined in any mesh system. The details of the TLLBM can be found in [10]. A basic description of the TLLBM is given below.

The two-dimensional, standard LBE with BGK approximation can be written as

$$f_i(x+e_{ix}\delta t, y+e_{iy}\delta t, t+\delta t) = f_i(x,y,t) + \frac{f_i^{\mathrm{eq}}(x,y,t) - f_i(x,y,t)}{(\tau+\delta t/2)}, \quad i=0,1,\ldots,N, \tag{1}$$

where τ is the single relaxation time, the extra term $\delta t/2$ added to τ compensates for the leading-order truncation error

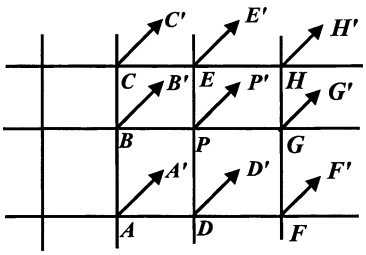

FIG. 1. Configuration of particle movement along the *i* direction.

during the Chapman-Enskog expansion, f_i is the distribution function along the *i* direction, f_i^{eq} is its corresponding equilibrium state, δt is the time step, $\mathbf{e}_i(e_{ix},e_{iy})$ is the particle velocity in the *i* direction, and *N* is the number of discrete particle velocities.

Suppose that a particle is initially at the grid point (x,y,t). Along the *i* direction, this particle will stream to the position $(x+e_{ix}\delta t,y+e_{iy}\delta t,t+\delta t)$. For a uniform lattice, $\delta x=e_{ix}\delta t$ and $\delta y=e_{iy}\delta t$. So $(x+e_{ix}\delta t,y+e_{iy}\delta t)$ is on the grid point. In other words, Eq. (1) can be used to update the distribution functions exactly at the grid points. However, for a nonuniform grid, $(x+e_{ix}\delta t,y+e_{iy}\delta t)$ is usually not at the grid point $(x+\delta x,y+\delta y)$. In the numerical simulation, only the distribution function at the mesh points for all time levels is needed, so that the macroscopic properties such as the density, flow velocity, and temperature can be evaluated at every mesh point. To get the distribution function at the grid point $(x+\delta x,y+\delta y)$ and the time level $t+\delta t$, the Taylor series expansion in the spatial direction is applied.

As shown in Fig. 1, for simplicity, the point *A* represents the grid point (x_A,y_A,t), point A' represents the position $(x_A+e_{ix}\delta t,y_A+e_{iy}\delta t,t+\delta t)$, and point *P* represent the position $(x_P,y_P,t+\delta t)$ with $x_P=x_A+\delta x$ and $y_P=y_A+\delta y$. So Eq. (1) gives

$$f_i(A',t+\delta t)=f_i(A,t)+\lfloor f_i^{\mathrm{eq}}(A,t)-f_i(A,t)\rfloor/\tau. \tag{2}$$

For the general case, A' may not coincide with the mesh point *P*. We truncate the Taylor series expansion to the second-order derivative terms. So $f_i(A',t+\delta t)$ can be approximated by the corresponding function and its derivatives at the mesh point *P* as

$$\begin{aligned} f_i(A',t+\delta t)=f_i(P,t+\delta t)&+\Delta x_A\frac{\partial f_i(P,t+\delta t)}{\partial x}\\ &+\Delta y_A\frac{\partial f_i(P,t+\delta t)}{\partial y}\\ &+\frac{1}{2}(\Delta x_A)^2\frac{\partial^2 f_i(P,t+\delta t)}{\partial x^2}\\ &+\frac{1}{2}(\Delta y_A)^2\frac{\partial^2 f_i(P,t+\delta t)}{\partial y^2}\\ &+\Delta x_A\Delta y_A\frac{\partial^2 f_i(P,t+\delta t)}{\partial x\,\partial y}\\ &+O[(\Delta x_A)^3,(\Delta y_A)^3], \end{aligned} \tag{3}$$

where $\Delta x_A=x_A+e_{ix}\delta t-x_P$ and $\Delta y_A=y_A+e_{iy}\delta t-y_P$. For the two-dimensional case, this expansion involves six unknowns: that is, one distribution function at the time level $t+\delta t$, two first order derivatives, and three second-order derivatives. To solve for these unknowns, six equations are needed to close the system. This can be done by applying the second-order Taylor series expansion at six points: *P,A,B,C,D,E*. As shown in [10], the following equation system can be obtained:

$$f_k'=\{s_k\}^T\{W\}=\sum_{j=1}^{6}s_{k,j}W_j,\quad k=P,A,B,C,D,E, \tag{4}$$

where

$$f_k'=f_i(x_k,y_k,t)+\lfloor f_i^{\mathrm{eq}}(x_k,y_k,t)-f_i(x_k,y_k,t)\rfloor/\tau+\delta t/2,$$

$$\{s_k\}^T=\{1,\Delta x_k,\Delta y_k,(\Delta x_k)^2/2,(\Delta y_k)^2/2,\Delta x_k\Delta y_k\},$$

$$\{W\}=\{f_i,\partial f_i/\partial x,\partial f_i/\partial y,\partial^2 f_i/\partial x^2,\partial^2 f_i/\partial^2 y,\partial^2 f_i/\partial x\,\partial y\}^T.$$

Our target is to find the first element $W_1=f_i(P,t+\delta t)$. Equation system (4) can be put into the following matrix form:

$$[S]\{W\}=\{f'\}. \tag{5}$$

In practical applications, it was found that the matrix $[S]$ might be singular or ill conditioned using only six points (*P,A,B,C,D,E*). To overcome this difficulty and make the method more general, more points are added and the least-squares approach [11] was introduced to optimize the over-constrained approximation by Eq. (5). As a result, the equation system for $\{\mathbf{W}\}$ becomes

$$\{W\}=([S]^T[S])^{-1}[S]^T\{f'\}=[A]\{f'\}. \tag{6}$$

From Eq. (6), we can have

$$f_i(x_0,y_0,t+\delta t)=W_1=\sum_{k=1}^{M}a_{1,k}f_k', \tag{7}$$

where $a_{1,k}$ are the elements of the first row of the matrix $[A]$, which is determined by the coordinates of mesh points, the particle velocity, and time step size, and will not be changed in the calculation procedure. *M* is the number of the points used and should be greater than 6. In the present study, a structured grid is used, and *M* is taken as 9. This means that for a reference mesh point *P*, we need to select its eight neighboring points to compute the coefficients in Eq. (7). Figure 1 shows the actual point distribution used in the present study. Although it is illustrated along the particle direction of 45°, the point distribution shown in Fig. 1 can be applied to other particle directions including the horizontal and vertical directions. We can calculate the coefficients in

Eq. (7) once and store them in advance, so little computational effort is introduced as compared with the standard LBE. On the other hand, Eq. (7) has nothing to do with the mesh structure. It only needs the information of coordinates of the mesh points. Thus we can say that Eq. (7) can be consistently used to any kind of mesh structure. But we have to indicate that, as compared to the standard LBE, the present method requires much more memory to store the coefficients $a_{1,k}$.

B. Thermal model

A thermal model was proposed by He *et al.* [12] recently. This model introduces an internal energy density distribution function to simulate the temperature field. The macroscopic density and velocity fields are still simulated using the density distribution function. The details of this thermal model can be found in [12]. A basic description is given below.

The density distribution function and energy density distribution function satisfy the following equations, respectively:

$$\partial_t f_i + (\mathbf{e}_i \cdot \nabla) f_i = -\frac{f_i - f_i^{\mathrm{eq}}}{\tau_\nu} + F_i, \tag{8}$$

$$\partial_t g_i + (\mathbf{e}_i \cdot \nabla) g_i = -\frac{g_i - g_i^{\mathrm{eq}}}{\tau_c} - f_i(\mathbf{e}_i - \mathbf{V}) \cdot [\partial_t \mathbf{V} + (\mathbf{e}_i \cdot \nabla)\mathbf{V}], \tag{9}$$

where

$$F_i = \frac{\mathbf{G} \cdot (\mathbf{e}_i - \mathbf{V})}{RT} f_i^{\mathrm{eq}}$$

and **G** is the external force acting on the unit mass. By adopting a second-order strategy to integrate the above two equations, one can get

$$\overline{f}_i(\mathbf{x} + \mathbf{e}_i \delta t, t + \delta t) - \overline{f}_i(\mathbf{x}, t) = -\frac{\delta t}{\tau_\nu + 0.5\delta t}[\overline{f}_i(\mathbf{x}, t) - f_i^{\mathrm{eq}}(\mathbf{x}, t)] + \frac{\tau_\nu F_i \delta t}{\tau_\nu + 0.5\delta t}, \tag{10}$$

$$\overline{g}_i(\mathbf{x} + \mathbf{e}_i \delta t, \mathbf{e}_i, t + \delta t) - \overline{g}_i(\mathbf{x}, \mathbf{e}_i, t) = -\frac{\delta t}{\tau_c + 0.5\delta t}[\overline{g}_i(\mathbf{x}, \mathbf{e}_i, t) - g_i^{\mathrm{eq}}(\mathbf{x}, \mathbf{e}_i, t)] - \frac{\tau_c}{\tau_c + 0.5\delta t} f_i(\mathbf{x}, \mathbf{e}_i, t) q(\mathbf{x}, \mathbf{e}_i, t)\, \delta t, \tag{11}$$

where

$$\overline{f}_i = f_i + \frac{\delta t}{2\tau_\nu}(f_i - f_i^{\mathrm{eq}}) - \frac{\delta t}{2} F_i,$$

$$\overline{g}_i = g_i + \frac{\delta t}{2\tau_c}(g_i - g_i^{\mathrm{eq}}) + \frac{\delta t}{2} f_i q_i,$$

$$q_i = (\mathbf{e}_i - \mathbf{V}) \cdot \left[\frac{1}{\rho}(-\nabla p + \nabla \cdot \mathbf{\Pi}) + (\mathbf{e}_i - \mathbf{V}) \cdot \nabla \mathbf{V}\right].$$

Then the macroscopic density, velocity, and internal energy can be calculated by

$$\rho = \sum_i \overline{f}_i, \tag{12a}$$

$$\rho \mathbf{V} = \sum_i \mathbf{e}_i \overline{f}_i + \frac{\rho \mathbf{G}\, \delta t}{2}, \tag{12b}$$

$$\rho \varepsilon = \sum_i \overline{g}_i - \frac{\delta t}{2} \sum_i f_i q_i. \tag{12c}$$

In this paper, the same nine-speed model is used as in [12]. The kinematic viscosity υ is related to the first relaxation time by $\upsilon = \tau_\nu RT$, and the thermal diffusivity χ is related to the second relaxation time by $\chi = \tau_c RT$

When this thermal model is implemented for flows with arbitrary geometry, Eqs. (10) and (11) cannot be used directly. In order to solve this problem, by applying the Taylor-series-expansion and least-squares approaches to these two equations, we can get

$$\overline{f}_i(x_0, y_0, t + \delta t) = V_1 = \sum_{k=1}^{M} a_{1,k} \overline{f_k'}, \tag{13}$$

$$\overline{g}_i(x_0, y_0, t + \delta t) = V_1' = \sum_{k=1}^{M} a_{1,k}' \overline{g_k'}, \tag{14}$$

where

$$\overline{f_k'} = \left(1 - \frac{\delta t}{\tau_\nu + 0.5\delta t}\right) f_i(x_k, y_k, \mathbf{e}_i, t) + \frac{\delta t}{\tau_\nu + 0.5\delta t} f_\alpha^{\mathrm{eq}}(x_k, y_k, \mathbf{e}_i, t) + \frac{\tau_\nu F_i \delta t}{\tau_\nu + 0.5\delta t},$$

$$\overline{g_k'} = \left(1 - \frac{\delta t}{\tau_c + 0.5\delta t}\right) g_i(x_k, y_k, \mathbf{e}_i, t) + \frac{\delta t}{\tau_c + 0.5\delta t} g_\alpha^{\mathrm{eq}}(x_k, y_k, \mathbf{e}_i, t) - \frac{\tau_c f_i q_i \delta t}{\tau_c + 0.5\delta t},$$

$$\{V'\} = \{g_i, \partial g_i/\partial x, \partial g_i/\partial y, \partial^2 g_i/\partial x^2, \partial^2 g_i/\partial^2 y, \partial^2 g_i/\partial x\, \partial y\}^T.$$

When we choose the same particle velocity model and the same surrounding points, the geometric matrices A and A' are the same for both the density distribution function and energy density distribution function, which can save both computational time and storage space. In this paper, we choose the same nine-speed model and the same eight sur-

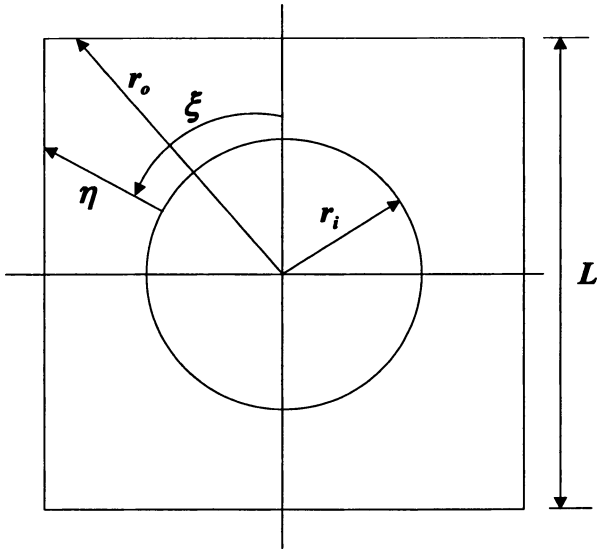

FIG. 2. Sketch of the physical domain.

rounding points for a reference mesh point P to compute the coefficients in Eqs. (13) and (14), respectively.

III. SIMULATION OF NATURAL CONVECTION IN A CONCENTRIC ANNULUS BETWEEN AN OUTER SQUARE CYLINDER AND AN INNER CIRCULAR CYLINDER

A. Problem definition and boundary condition

A schematic view of a horizontal concentric annulus between a square outer cylinder and a heated circular inner cylinder is shown in Fig. 2. Heat is generated uniformly within the circular inner cylinder, which is placed concentrically within the cold square cylinder. For the present computation, a nonuniform mesh is used, where mesh points are stretched near the wall to capture the thin boundary layer. In the middle part of the flow field, the mesh is relatively coarse since the velocity and temperature gradients are not very large in this region.

Based on the Boussinesq approximation, the effective external force can be written as

$$\rho \mathbf{G} = \rho \beta g_0 (T - T_m)\mathbf{j}, \tag{15}$$

where β is the thermal expansion coefficient, g_0 is the acceleration due to gravity, and $\mathbf{j}$ is the vertical direction opposite to that of gravity. $T_m = (T_i + T_o)/2$ is the average temperature, in which T_i is the temperature on the inner (hot) wall and T_o is the temperature on the outer (cold) wall. The prandtl number is defined as $N_{\mathrm{Pr}} = \nu/\chi$, and the Rayleigh number is defined as $N_{\mathrm{Ra}} = \beta \Delta T g_0 L^3/\nu\chi$.

For the natural convection problem, $\sqrt{\beta g_0 \Delta T L}$ is the characteristic velocity, where $\Delta T = T_i - T_o$. To ensure the code working properly in the near-incompressible regime, we carefully choose the value of $\sqrt{\beta g_0 \Delta T L}$. It is chosen to be $0.1c$ at low Rayleigh number and $0.15c$ at high Rayleigh number. This means that the Mach number is 0.1 at low Rayleigh number and 0.15 at high Rayleigh number. Once $\beta g_0 \Delta T L$ is determined, the kinematic viscosity and the thermal diffusivity are determined through the two dimensionless numbers N_{Pr} and N_{Ra}, respectively. By using the relationship between the kinematic viscosity, the thermal diffusivity, and the two relaxation times, the two relaxation times τ_ν and τ_c can be easily determined.

Generally speaking, the problem of formulating boundary conditions within the LBE formalism consists of finding an appropriate relation, which expresses the incoming from outside environment to the flow field (unknown) as a function of the outgoing from the flow field to the outside environment (known). The bounce-back rule of the nonequilibrium distribution is such a way and is used here to determine the unknowns from the known functions. As shown in Ref. [12], for isothermal problems, the following hydrodynamic boundary condition for the density distribution function can be used:

$$f_\alpha^{\mathrm{neq,iso}} = f_\beta^{\mathrm{neq,iso}}, \tag{16}$$

where α and β have the opposite direction, β represents outgoing direction, and α represents the corresponding opposite incoming direction. For thermal problems, the thermodynamic Dirichlet boundary condition can be represented by the energy density distribution function, which is written as

$$g_\alpha^{\mathrm{neq}} - e_\alpha^2 f_\alpha^{\mathrm{neq,iso}} = -(g_\beta^{\mathrm{neq}} - e_\beta^2 f_\beta^{\mathrm{neq,iso}}). \tag{17}$$

Since the density distribution in the LBE thermal model does not take into account the temperature variation, its nonequilibrium part satisfies the boundary condition (16) and plays the role of $f^{\mathrm{neq,iso}}$ in the boundary condition (17).

For the inner circular cylinder, the outgoing population at a boundary point can be determined by the condition of $\mathbf{e}\cdot\mathbf{n} < 0$, where $\mathbf{n}$ is the outward vector normal to the boundary. Incoming populations are defined by the condition of $\mathbf{e}\cdot\mathbf{n} \geqslant 0$. For the outer square cylinder, the outgoing populations are defined by the condition of $\mathbf{e}\cdot\mathbf{n} > 0$, while the incoming populations are defined by $\mathbf{e}\cdot\mathbf{n} \leqslant 0$. For the outgoing distributions, their values can be determined by Eqs. (13) and (14). In contrast, the incoming distributions are determined by the boundary conditions (16) and (17). Some other implementation of boundary conditions on the curved boundary can be found in the work of Mei *et al.* [13].

B. Definition of Nusselt numbers

The local heat transfer rate on the inner cylinder can be computed by

$$q = h(T_i^* - T_o^*) = -k\frac{\partial T^*}{\partial n}, \tag{18}$$

where T^* is the dimensional temperature, T_i^* and T_o^* are, respectively, the temperature on the inner and outer walls, h represents the local heat transfer coefficient, and k is the thermal conductivity, $k = \rho c_p \chi$. From Eq. (18), we can get

TABLE I. Comparison of $\overline{N}_{\mathrm{Nu}}$.

			$\overline{N}_{\mathrm{Nu}}$		
Cases	rr	N_{Ra}	Present	Shu and Zhu [15]	Moukalled and Acharya [14]
1	5.0	10^4	2.08	2.08	2.071
2	2.5		3.24	3.24	3.331
3	1.67		5.39	5.40	5.826
4	5.0	10^5	3.79	3.79	3.825
5	2.5		4.84	4.86	5.08
6	1.67		6.20	6.21	6.212
7	5.0	10^6	5.96	6.11	6.107
8	2.5		8.75	8.90	9.374
9	1.67		11.65	12.00	11.62

$$h=-k\frac{\partial T}{\partial n}. \tag{19}$$

Here T is the nondimensional temperature, which is defined as $T=(T^*-T_o^*)/(T_i^*-T_o^*)$ and $\partial T/\partial n$ is the temperature gradient in the direction normal to the boundary.

Since at steady state the Nusselt numbers along the inner and outer walls are the same, there is no need to pay separate attention to the average Nusselt numbers for the outer and inner boundaries. The average Nusselt numbers for the inner boundary is determined by

$$\overline{N}_{\mathrm{Nu}}=\frac{\overline{hS}}{k}=\frac{\overline{\partial T}}{\partial n}S, \tag{20}$$

where S is defined as half of the circumferential lengths of the inner cylinder surface due to the symmetry, in the same way as in the work of Moukalled and Acharya [14] for comparison, and $\overline{h}$ is the average heat flux across the boundary.

C. Validation of numerical results

As discussed before, most research work has focused on the study of natural convection in annuli between either concentric or eccentric circular cylinders. Only a few publications involved the study of natural convection in an annulus between an outer square cylinder and an inner circular cylinder. The work of Moukalled and Acharya [14] and Shu and Zhu [15] is among such studies. Moukalled and Acharya [14] solved the Navier-Stokes equations in a body-fitted coordinate system using a control volume-based numerical procedure. Their numerical data were validated by comparison with some experimental data and found to be in good agreement. Recently, the global method of differential quadrature (DQ) was applied by Shu and Zhu [15] to simulate this natural convection problem. Their work consists of the numerical results for Rayleigh numbers ranging from 10^4 to 10^6 and aspect ratios between 1.67 and 5.0. So in this study, both the results of Moukalled and Acharya [14] and the results of Shu and Zhu [15] are used to validate the present numerical results. The average Nusselt numbers $\overline{N}_{\mathrm{Nu}}$ calculated by three different methods are compared in Table I for Rayleigh numbers of 10^4, 10^5, and 10^6 and aspect ratios of 5.0, 2.5, and 1.67. It is noted that the reference length used in the Rayleigh number is the side length of the square cylinder, L. The mesh size used in the present study is, respectively, 101×161 for $N_{\mathrm{Ra}}=10^4$, 129×201 for $N_{\mathrm{Ra}}=10^5$, and 251×321 for $N_{\mathrm{Ra}}=10^6$. From Table I, it can be seen that at low Rayleigh numbers of 10^4 and 10^5, the three results compare very well with each other. And at high Rayleigh number of 10^6, there are some deviations between the present results and the reference data. But the maximum difference is within 2.5%. So we can say that the present results are very accurate, and the present method can be used to solve complex thermal problems accurately and effectively.

The flow and thermal fields for these nine cases are identical to those described previously in [15], which will not be repeated here.

IV. CONCLUSIONS

In this paper, the Taylor-series-expansion and least-squares-based lattice Boltzmann method was employed to extend the current thermal model to study the natural convection in a horizontal concentric annulus between a square outer cylinder and a circular inner cylinder, which is a complex thermal flow problem. Numerical results for Rayleigh numbers range from 10^4 to 10^6 and aspect ratios between 1.67 and 5.0 are presented, which agree well with available data in the literature. It is also found in this study that both the aspect ratio and the Rayleigh number are critical to the patterns of flow and thermal fields as shown in [15]. It should be indicated that the TLLBM used in this paper is basically a meshless approach and can be easily applied to any complex geometry and nonuniform grid. It is applicable for different physical domains including the eccentric case.

[1] S. Chen and G. D. Doolen, Annu. Rev. Fluid Mech. **30**, 329 (1998).
[2] N. Cao, S. Chen, S. Jin, and D. Martinez, Phys. Rev. E **55**, R21 (1997).
[3] S. Succi, G. Amati, and R. Benzi, J. Stat. Phys. **81**, 5 (1995).
[4] H. Chen, Phys. Rev. E **58**, 3955 (1998).
[5] G. Peng, H. Xi, and C. Duncan, Phys. Rev. E **58**, 4124 (1998).
[6] G. Peng, H. Xi, and C. Duncan, Phys. Rev. E **59**, 4675 (1999).
[7] H. Xi, G. Peng, and S. Chou, Phys. Rev. E **59**, 6202 (1999).
[8] H. Xi, G. Peng, and S. Chou, Phys. Rev. E **60**, 3380 (1999).
[9] X. He, L.-S. Luo, and M. Dembo, J. Comput. Phys. **129**, 357 (1996).
[10] C. Shu, Y. T. Chew, and X. D. Niu, Phys. Rev. E **64**, 045701 (2001).
[11] G. H. Golub and C. F. Van Loan, *Matrix Computations*, 3rd ed. (Johns Hopkins University Press, Balimore, MD, 1996).

[12] X. He, S. Chen, and G. Doolen, J. Comput. Phys. **146**, 282 (1998).
[13] R. Mei, L.-S. Luo, and W. Shyy, J. Comput. Phys. **155**, 307 (1999).
[14] F. Moukalled and S. Acharya, J. Thermophys. Heat Transfer **10**(3), 524 (1996).
[15] C. Shu and Y. Zhu, Int. J. Numer. Methods Fluids **38**, 429 (2002).